ACTA SOCIETATIS
BOTANICORUM POLONIAE
Vol. XLVIII, nr 3:423—441
1979

# Modeling of growth in shoot apical dome

Z. HEJNOWICZ and J. NAKIELSKI

Department of Biophysics and Cell Biology, Silesian University

(Received: March 7, 1979)

Abstract

The vectorial field of displacement velocities $\underline{V}$ in growing apical dome is calculated from the scalar field adjusted to the geometry of the dome and to different variants of the distribution of linear growth rate along axis. The distribution of growth rate in volume and the temporal course of cell wall net deformation in the apical dome calculated from the $\underline{V}$ fit within the range of empirical data when the linear growth rate along the axis increases with distance from the tip. The distribution of volume growth rate attains the minimum inside the distal region of the dome where the zone of central mother cells occurs.

## INTRODUCTION

In the apical meristem the growth rates in different parts are strictly interrelated so that no cell can migrate past the others and all grow compatibly. Direct measurement of these rates is difficult, if possible at all inside the meristem. Among indirect methods, determination of mitotic indices in different parts of the meristem seems to be most rational and simplest, However, this method is based on the assumption that the duration of mitosis is constant, even if the duration of the whole mitotic cycle is not, in different parts of the meristem. This paper shows how the distribution of growth rates—linear in different directions, in surface area in different planes, and volumetric—can be calculated on the basis of the geometry of the apical meristem and the distribution of linear growth rates along the axis or along one meridional line on the dome surface, according to the concept of the scalar field from which the vectorial field of displacement velocities can be obtained (Hejnowicz, 1980). This is done for a model of an apical dome in the form of a figure of revolution, described in cylindrical coordinates r, z, $\varphi$. The calculations are aimed at determining the distribution of:

1. linear growth in different main directions (periclinal, anticlinal, radial, latitudinal);

2. growth in area at dome surface, in axial, and in transverse planes;
3. growth in volume;
4. temporal course of expansion.

We explore two possible approaches to the model: analytical when the geometry is given in analytical form, and graphical when it is in graphical form only.

## 1. Vector and scalar fields considered

Growth causes displacement of identifiable elements of the cell wall network in respect to a reference element in a plant organ. To each point of the network, which for our purpose may be considered as a continuum, a vector of displacement velocity $\underset{\sim}{V}$ can be associated so that the field $\underset{\sim}{V}(r, z)$ is differentiable. In the case of an apex, this field is steady or nearly so, if the reference element is chosen at its summit.

Through every point of the apex a displacement line, defined by a parameter c, and an orthogonal trajectory to the displacement lines can be drawn. On a particular orthogonal trajectory the parameter c changes from 0 on the axis to some maximum value on the surface. If the pattern of displacement lines does not change in time, i.e. it is steady, the lines are identical with element paths. Only such a case will be considered in this paper. Since our aim is to show the principles of the modeling work, we assume that also the shape of the dome is stationary, i.e. the dome (open at its basis at the level at which leaf primordia emerge in the case of shoot apex) does not change its shape during growth, this meaning that its surface is

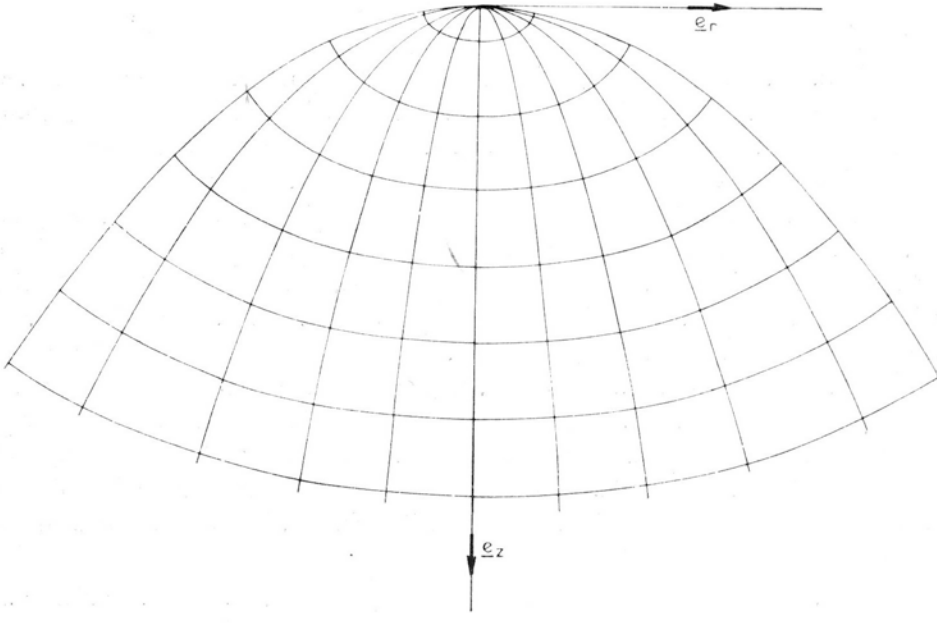


Fig. 1. Model of apical dome with displacement lines and their orthogonal trajectories

tangent to the displacement lines. There are good reasons to consider that the elements which are on the trajectory orthogonal to the displacement lines at a particular moment, remain on this trajectory during subsequent growth (Hejnowicz, 1980). The present paper assumes this type of growth, which be called growth preserving the orthogonality of periclinal and anticlinal walls (GPO).

Fig. 1 illustrates the geometry used in this paper. Let us introduce a unit vector $\underline{e}_m$ tangent to the displacement line at a given point, and the magnitude of the vector $\underline{V}$ at point—$|\underline{V}|$. The field $\underline{V}$ (r, z) can be put in the form $\underline{V}(r, z)=\underline{e}_m(r, z) \cdot |V(r, z)|$. The field $\underline{e}_m$ (r, z) defines the pattern of displacement lines. It belongs to the geometry of the apex. If we assume a certain $|\underline{V}|$ along one displacement line, for instance along the axis, then for the given geometry the whole field $\underline{V}$ (r, z) is already defined. We shall assume different $|\underline{V}|$ along the axis and will calculate the corresponding distribution of growth rates.

In the case of GPO, the field $\underline{V}$ (r, z) can be represented by a function of the gradient of some scalar field G (r, z) such that on the axis

$$\underline{V}(0, z)\equiv\underline{V}(z_o)=\underline{\text{grad}}\, G(z_o) \quad \text{while in general:}$$

$$\underline{V}(r, z)=\mu(r, z)\ \underline{\text{grad}}\ G(r, z) \tag{1}$$

and

$$\mu(r, z)=\frac{|\underline{\text{grad}}\, G_{c=a}|^2}{|\underline{\text{grad}}\, G_{c=o}|^2} \tag{2}$$

where $\underline{\text{grad}}\, G_{c=a}$ is the gradient of G at point P (r, z) through which the displacement line defined by the parameter c=a runs, and $\underline{\text{grad}}\, G_{c=0}$ is the gradient of G on the axis at intersection with the orthogonal trajectory which runs through point P (Hejnowicz 1980). In this formulation the displacement lines are the field lines of $\underline{V}$ while the orthogonal trajectories of displacement lines are the equipotential lines of G (i.e. lines on the (rz) plane such that at each line G is constant).

## 2. Growth rates

The knowledge of the vectorical field of displacement velocity of elements is of primary importance for analysis of growth patterns (Erickson, 1976; Hejnowicz, 1980).

The relative elemental rate of growth, RERG, of segment l oriented in the direction of the unit vector $\underline{e}_s$, $RERG_{l(s)}$ is:

$$RERG_{l(s)}=\underline{\text{grad}}\,(\underline{V}\cdot\underline{e}_s)\cdot\underline{e}_s \tag{3}$$

An organ which is a figure of revolution, grow without twisting, so that vectors $\underline{V}$ lie in axial planes and the unit vector $\underline{e}_s$ is either in axial or orthogonal to this plane:

$$RERG_{l(s)} = \frac{\partial V_r}{\partial r}\cos^2\alpha + \frac{\partial V_z}{\partial z}\cos^2\beta + \\ + \cos\alpha\cos\beta\left(\frac{\partial V_r}{\partial z} + \frac{\partial V_z}{\partial r}\right) + \frac{V_r}{r}\cos^2\gamma \qquad (4)$$

where $\cos\alpha$, $\cos\beta$, $\cos\gamma$ are direction cosines of $\underline{e}_s$ in respects to the base unit vectors $\underline{e}_r$, $\underline{e}_z$, $\underline{e}_\varphi$ respectively (on the condition that $\cos\varphi$ attains either value 0 or 1 as mentioned previously). In particular:

1. along the pericline (along displacement line), $\cos\alpha = \sin\beta$, $\gamma = 90°$, Fig 2a

$$RERG_{l(per)} = \frac{\partial V_r}{\partial r}\sin^2\beta + \frac{\partial V_z}{\partial z}\cos^2\beta + \cos\beta\sin\beta\left(\frac{\partial V_r}{\partial z} + \frac{\partial V_z}{\partial r}\right) \qquad (5)$$

where $\beta$ is the angle between the displacement line and the z-axis;

2. along the anticline (along an orthogonal to the displacement lines), $\cos\beta = -\sin\alpha$, $\gamma = 90°$

$$RERG_{l(ant)} = \frac{\partial V_z}{\partial z}\sin^2\alpha + \frac{\partial V_r}{\partial r}\cos^2\alpha - \cos\alpha\sin\alpha\left(\frac{\partial V_r}{\partial z} + \frac{\partial V_z}{\partial r}\right) \qquad (6)$$

where $\alpha$ is the angle between the orthogonal trajectory and $\underline{e}_r$;

3. along the radius $RERG_{l(r)} = \frac{\partial V_r}{\partial r}$; (7)

4. along the axis $RERG_{l(z)} = \frac{\partial V_z}{\partial z}$; (8)

5. along the latitude $RERG_{l(lat)} = \frac{V_r}{r}$; (9)

The relative elemental rate of growth in area $RERG_a$ in the plane defined by two orthogonal unit vectors $\underline{e}_{s1}$ and $\underline{e}_{s2}$ at a given point is the sum of linear $RERG_l$ in these directions:

$$RERG_a = RERG_{l(s1)} + RERG_{l(s2)}$$

In particular:

1. in axial plane we take $RERG_l$ in the directions of $\underline{e}_r$ and $\underline{e}_z$

$$RERG_{a(axial)} = \frac{\partial V_r}{\partial r} + \frac{\partial V_z}{\partial z} \qquad (10)$$

2. in transverse plane we take $RERG_l$ in the direction of $\underline{e}_r$ and $\underline{e}$

$$RERG_{a(trans)} = \frac{\partial V_r}{\partial r} + \frac{V_r}{r} \qquad (11)$$

3. on the organ surface we take $RERG_1$ along the pericline (meridian) and along the latitude

$$RERG_{a\,(tangent)} = \frac{\partial V_r}{\partial r}\sin^2\beta + \frac{\partial V_z}{\partial z}\cos^2\beta + \sin\beta\cos\beta\left(\frac{\partial V_r}{\partial z}+\frac{\partial V_z}{\partial r}\right)+\frac{V_r}{r} \qquad (12)$$

where $\beta$ is the angle between the displacement line (meridian) and $\underline{e}_z$;

4. on the surface orthogonal to the displacement lines we take $RERG_1$ along the anticline and along the latitude

$$RERG_{a\,(ort)} = \frac{\partial V_r}{\partial r}\cos^2\alpha + \frac{\partial V_z}{\partial z}\sin^2\alpha - \sin\alpha\cos\alpha\left(\frac{\partial V_r}{\partial z}+\frac{\partial V_z}{\partial r}\right)+\frac{V_r}{r} \qquad (13)$$

where $\alpha$ is the angle between the orthogonal trajectory and $\underline{e}_r$.

The relative rate of growth in volume is the sum of linear rates in three orthogonal directions at a given point

$$RERG_{vol} = RERG_{11} + RERG_{12} + RERG_{13} \qquad (14)$$

It is convenient to take $l_1, l_2, l_3$ parallel to base vectors. The right side of (14) is the divergence of vector field V, thus $RERG_{vol} = \mathrm{div}\,\underline{V}$. This is valid for all orthogonal coordinate systems because the operator div is an invariant. In cylindrical coordinated, for a figure of revolution

$$RERG_{vol} = \frac{\partial V_z}{\partial z} + \frac{1}{r}\frac{\partial}{\partial r}(r\cdot V_r) \qquad (14a)$$

## 3. Temporal course of dome expansion

The definition of displacement velocity along the axis is $|\underline{V}| = \frac{dz}{dt}$. We can thus write for the elements lying and being displaced along the axis: $dz = |\underline{V}(z)|\,dt$ or, after separation of variables, $\frac{dz}{|\underline{V}(z)|} = dt$

$$\text{Hence} \int \frac{dz}{|\underline{V}(z)|} = t - t_0 \qquad (15)$$

This equation gives the displacement of any element located at $z_0$ at instant $t_0$ during the time interval $t - t_0$ along the z-axis.To get the displacement for elements beyond the z-axis, an element should be displaced along its displacement line from position $P_0$ at instant $t_0$ to the intersection with the orthogonal trajectory on which is located at instant t the axial element which at instant $t_0$ lay on the orthogonal trajectory passing through $P_0$.

## 4. Analytical approach to the model

Let us assume that the family of displacement lines is described by the equation $r=a\,f(z)$, where a changes from zero on the z-axis to $a_{max}$ on the organ surface. The differential equation for the family is $\frac{dr}{dz}=\frac{rf'(z)}{f(z)}$ and for the family of orthogonal trajectories of the displacement lines $\frac{dr}{dz}=-\frac{f(z)}{rf'(z)}$

The solution of this equation gives the equation for the trajectory which crosses the axis at $z_0$: $\frac{1}{2}r^2+F(z)-F(z_0)=0$ where $F(z)=\int\frac{f(z)}{f'(z)}dz$

With each point of the trajectory we associate the constant value of G defined by G as a continuous function of z along the z-axis $G=G(z_0)$.

$$\text{Thus } G=\frac{1}{2}r^2+F(z)+C(z_0) \tag{16}$$

On the axis we have $F(z_0)+C(z_0)=G(z_0)$

$$\text{hence } C(z_0)=G(z_0)-F(z_0) \tag{17}$$

Since $G(z_0)$ is a monotonic function, there exists an inverse function to it, $z_0=z_0(G)$. Introducing this into (17) we obtain C as a function of G, $C=C(G)$, which introduced into (16) yields G as a function of r and z, $G=G(r,z)$. Having G in analytical form one can calculate the gradient of G and then $\underline{V}$ according to (1) at each point of the dome. Components of the vector $\underline{V}$ in the r and z directions are: $V_r=\frac{\partial G}{\partial r}$, $V_z=\frac{\partial G}{\partial z}$

## 5. Graphical approach to the model

Having a pattern of displacement lines we can draw their orthogonal trajectories creating in this way an orthogonal net. Let us assume that we know the distribution of linear RERG along the axis. Integrating it twice we obtain $G(z_0)$. Orthogonal trajectories of displacement lines are equipotential lines of the scalar field G, thus the value of $G(z_0)$ is valid for all points of the orthogonal trajectory which intersects the axis at $z_0$. Determination of the derivatives of $\underline{V}$ is thus reduced to determination of the surface G(r, z) and its differentiation, which can be done in two ways:

A. Numerical smoothing of the values G(r, z) given originally at the intersection of straight lines parallel and orthogonal to the z-axis with successive equipotential lines along the straight lines and numerical calculation of the second derivative: $\frac{\partial^2 G}{\partial r^2}$, $\frac{\partial^2 G}{\partial z^2}$, $\frac{\partial^2 G}{\partial r\,\partial z}$

This method might be adapted for an electronic computer by using smoothing--differentiating formulas such as those described by Erickson (1965, 1976).

B. Calculation of $\underline{V}(r, z)$ on the basis of geometry of the orthogonal net and graphical differentiation of $\underline{V}$. This method was used in the preparation of the present paper, so it is described in detail. First we utilise the property of $|\underline{\text{grad}}\ G|$ which is inversely proportional to the distance between two equipotential lines G and $G+\Delta G$. From (1) and (2) we have thus

$$|\underline{V}| = \left(\frac{\Delta m_a}{\Delta m_o}\right)^2 |\underline{\text{grad}}\ G| = \left(\frac{\Delta m_a}{\Delta m_o}\right)^2 \frac{\Delta m_o}{\Delta m_a} |\underline{\text{grad}}\ G_0| = \frac{\Delta m_a}{\Delta m_o} |\underline{V}_0| \qquad (1b)$$

where $\Delta m_a$ and $\Delta m_o$ are the distances between neighbouring orthogonal trajectories of displacement lines, embracing point P measured along the displacement lines a and the axis respectively, and $V_0$ is $\frac{\partial G}{\partial z}$ at the intersection of the equipotential line running through point P with the axis. The periclinal $RERG_1$ (between points $P_1$ and $P_2$ lying on the same displacement line a) (Fig. 2 A) is:

$$RERG_{1\,(per)} \simeq \frac{1}{\Delta m_a} (|\underline{V}_{a2}| - |\underline{V}_{a1}|) \qquad (18)$$

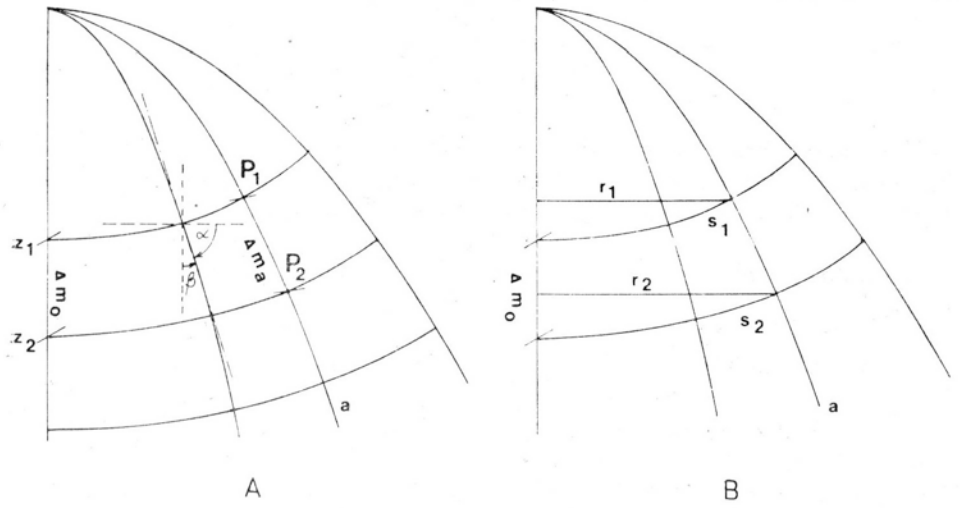


Fig. 2 Explanation to the calculation of linear growth rate:
A — in periclinal direction (along displacement lines); B — in anticlinal direction (along orthogonal trajectory of displacement lines). See text.

where $|\underline{V}_{a1}|$ and $|\underline{V}_{a2}|$ are the values of $\underline{V}$ at points $P_1$ and $P_2$ and $\Delta m_a$ is the distance between them. Applying (1b) we obtain

$$RERG_{1\,(per)} \simeq \frac{\left(\frac{\Delta m_a}{\Delta m_0}\right)_2 |\underline{V}_{02}| - \left(\frac{\Delta m_a}{\Delta m_0}\right)_1 |\underline{V}_{01}|}{\Delta m_a} \qquad (19)$$

where $|\underline{V}_{01}|$ and $|\underline{V}_{02}|$ concern the points $z_1$ and $z_2$ in Fig. 2A. The latter formula allows to calculate $RERG_{mer}$ if we know G along the axis and the distances $\Delta m$. Often the formula for $RERG_{1\,(per)}$ may be simplified. Let us expand $|\underline{V}_0|$ and $\frac{\Delta m_a}{\Delta m_0}$ using the first order terms only:

$$|\underline{V}_{02}|=|\underline{V}_{01}|+\frac{d|\underline{V}_0|}{dm_0}\Delta m_0 \qquad \text{and} \qquad \left(\frac{\Delta m_a}{\Delta m_0}\right)_2=\left(\frac{\Delta m_a}{\Delta m_0}\right)_1+\frac{d\left(\frac{\Delta m_a}{\Delta m_0}\right)}{dm_a}\Delta m_a$$

Introducing this expansion into (19) we obtain

$$RERG_{1\,(per)}\simeq\frac{d|\underline{V}_0|}{dm_0}+\frac{d\left(\frac{\Delta m_a}{\Delta m_0}\right)}{dm_a}|\underline{V}_0|+\frac{d\left(\frac{\Delta m_a}{\Delta m_0}\right)}{dm_a}\Delta m_a$$

Often $\frac{d\left(\frac{\Delta m_a}{\Delta m_0}\right)}{dm_a}$ is very small, thus the two last terms on the right side may be neglected. $RERG_{1\,(per)}$ is then the same for all points on the orthogonal trajectory of displacement lines and is defined by $\frac{d|\underline{V}_0|}{dm_0}$ on the axis;

$$RERG_{1\,(per)}\simeq\frac{d|\underline{V}_0|}{dm_0} \tag{19a}$$

The relative elemental growth rate in the direction orthogonal to the displacement lines in the axial plane $RERG_{1\,(ant)}$ and in the plane orthogonal to the axial plane $RERG_{1\,(lat)}$ are defined by the increments of segments of the net in Fig. 2B expressed by the following formulas $RERG_{1\,(ant)}=\frac{S_2-S_1}{S_1\,\Delta t}$ $\qquad RERG_{1\,(lat)}=\frac{2\pi(r_2-r_1)}{2\pi r_1\,\Delta t}$

for small $\Delta t$ $\quad \Delta m_a=V_a\,\Delta t$

Using (1b) we obtain

$$RERG_{1\,(ant)}=\frac{\Delta S}{S\Delta m_0}|\underline{V}_0|, \qquad RERG_{1\,(lat)}=\frac{\Delta r}{r\,\Delta m_0}|\underline{V}_0| \tag{20a.b}$$

The formulas may be treated as final ones. Then $\Delta s$ and $\Delta r$ must be determined directly on the orthogonal net. However, $\Delta s$ and $\Delta r$ can be drawn in functional form and differentiated graphically. Then the formulas take the form:

$$RERG_{1\,(ant)}=|\underline{V}_0|\frac{d\ln s}{dm_0}, \qquad RERG_{1\,(lat)}=|\underline{V}_0|\frac{d\ln r}{dm_0}$$

## RESULTS

We have assumed for calculations a pattern of displacement lines in the form of a family of parabolas $r^2=az$. The line specified as $a=0$ is identical with the dome

axis, the line $a=a_{max}$ is its surface. The net of displacement lines and of their orthogonal trajectories is given in Fig. 1. The calculations have been done by the two methods. In the analytical one we use the equation of parabolas, in the graphical one — the geometric relations observed in the net. Comparison of the results obtained graphically with the rigorous results of analytical method allows to estimate, whether the graphical method is suitable in studies of real domes. Analytical and graphical methods are used with the same functions $G(z_0)$. Additionally we used the graphical method for a case in which the growth rate on the axis was defined graphically in a form which could not be described analytically.

## 1. Analytical approach

For parabolic displacement lines, $r^2=az$, the equation of their orthogonal trajectories is; $\frac{dr}{dz}=-\frac{2z}{r}$. By integrating we obtain $\frac{1}{2}r^2+z^2-z_0^2=0$ and according to (16) the field G is $G=\frac{1}{2}r^2+z^2+C(z_0)$.

Variant 1—The relative elemental growth rate along the axis is constant

$RERG_{1(z_0)}=c$ thus $G(z_0)=\frac{1}{2}cz_0^2$. For simplicity we adopt a time unit such that $c=1$. Now $G(z_0)=\frac{1}{2}z_0^2$ and $z_0=\sqrt{2G}$. $C(G)=G-2G=-G$, therefore $G=\frac{1}{4}r^2+\frac{1}{2}z^2$. Using (2) we obtain $\mu=\frac{2r^2+4z^2}{r^2+4z^2}$. One can prove easily that $\mu$ becomes unity on the axis (when $r=0$) except the very tip where it tends to attain the value 2. (Namely, introducing to the equation the relation $r^2=az$ we have $\lim_{z\to 0}\frac{2r^2+4z^2}{r^2+4z^2}=\lim_{z\to 0}\frac{2a+4z}{a+4z}=2$).

This means that the factor $\mu$ introduces some mathematical pecularities to the field $\underline{V}$ near the tip, and the values calculated as limits of functions of this field, when z approaches 0 may be unrealistic.

The components of the vector $\underline{V}$ are: $V_r=\frac{r^3+2rz^2}{r^2+4z^2}$ and $V_z=\frac{2r^2z+4z^3}{r^2+4z^2}$. The functions of the angle between the displacement line and the unit vector $\underline{e}_z$ are:

$$\cos\beta=\frac{2z}{\sqrt{r^2+4z^2}} \qquad \sin\beta=\frac{r}{\sqrt{r^2+4z^2}}.$$

Using the formulas (5—14) for growth rates we obtain:

$$RERG_{1(per)}=1-\frac{2r^2z^2}{(r^2+4z^2)^2}$$

$$RERG_{1(ant)}=1+\frac{r^4-8z^4}{(r^2+4z^2)^2}$$

$$RERG_{l\,(lat)} = \frac{r^2+2z^2}{r^2+4z^2}$$

$$RERG_{l\,(r)} = \frac{r^4+10r^2z^2+8z^4}{(r^2+4z^2)^2}$$

$$RERG_{vol} = \frac{4(r^4+5r^2z^2+8z^4)}{(r^2+4z^2)^2}$$

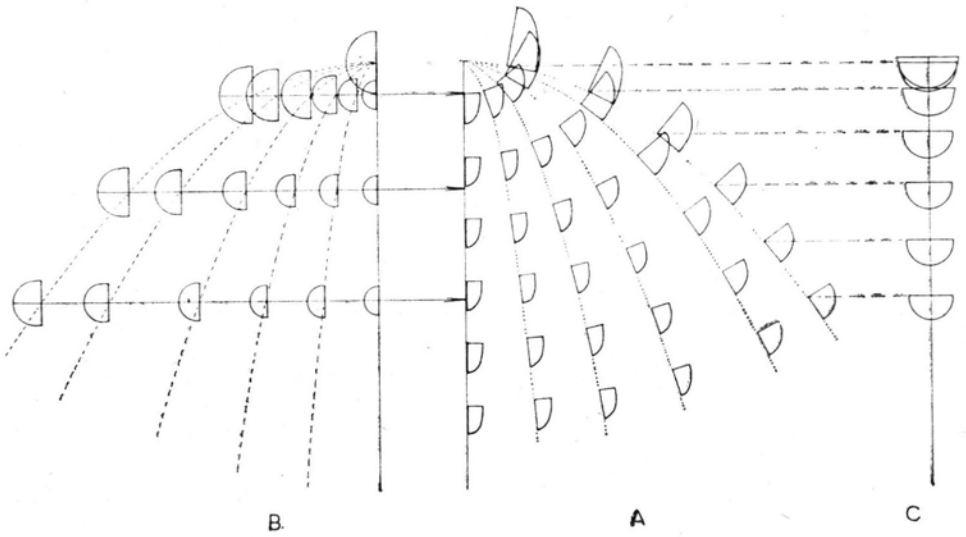


Fig. 3. Distribution of growth rates — linear and in area — obtained by analytical method for variant 1 characterized by constant linear growth rate along the axis

The linear growth rate in each direction at a certain point on a particular plane is given by the ellipse (circle) radius running from the point in this direction. The growth rate in area is proportional to ellipse surface area: A — in axial plane, at nodes of the net shown in Fig. 1; B — in transverse planes at the levels indicated by arrows; C — on the surface of the apical dome at the levels indicated by dashed lines

The results of calculations are summarized in Fig. 3. It is seen that the linear growth on the surface is nearly isotropic, i.e. the growth rate does not depend on the direction, However, it is not isogonic—there are slight changes in the rate as the distance from the tip increases. The growth in the axial plane is distinctly anisotropic in the central part but becomes almost isotropic in the peripheral part. Near the tip, at the periphery there is a higher growth rate in anticlinal than in periclinal direction. This anisotropy is connected to mathematical pecularities of the parabolic displacement lines (the course of the latter near the tip differs widely from that of the straight lines radiating from tip which can be expected in isotropic growth of tip region). Growth on the transverse plane is nearly isotropic, but not isogonic. The surface area of one half or one quarter of the ellipse (or circle) in Fig. 3 characterizes the surface growth rate in area in the indicated plane. Obviously, the deformation of the ellipse in relation to the circle characterizes the aniso-

tropy of growth. There is, in general a higher growth rate in the area at the periphery, especially in the apical part.

The distribution of the volume growth rate for the considered variation of growth is shown in Fig. 5A. This variant is characterized by a relatively lower volume growth rate in the core of the dome.

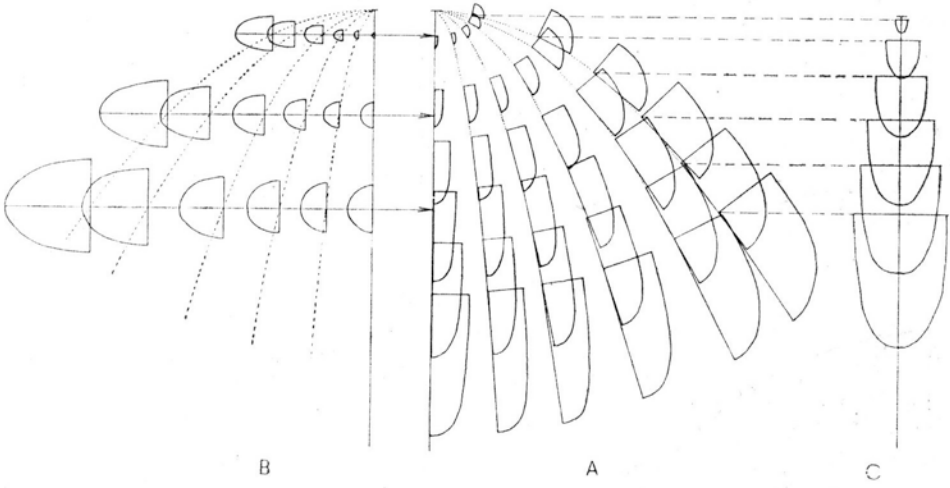


Fig. 4 Distribution of growth rate — linear and in area — obtained by analitical method for variant 2 characterized by growth rate along the axis, proportional to the distance from the tip: A — in axial plane; B — in transverse planes; C — on the surface of the apical dome. See Fig. 3

Variant 2—The relative elemental growth rate along the z-axis is proportional to the distance from the tip

$RERG_{1(z_0)}=cz$. Adopting the time unit so that $c=1$ we have $G(z_0)=\frac{1}{6}z_0^3$, and $C=G(z_0)-z_0^2=G-(6G)^{2/3}$. From (16) we obtain $G=\frac{1}{6}\left(\frac{1}{2}r^2+z^2\right)^{3/2}$. The components of the gradients of G are

$$\frac{\partial G}{\partial r}=\frac{1}{4}r\left(\frac{1}{2}r^2+z^2\right)^{1/2}, \qquad \frac{\partial G}{\partial z}=\frac{1}{2}z\left(\frac{1}{2}r^2+z^2\right)^{1/2}$$

The factor $\mu$ is the same as in the previous variant (obviously it can be calculated separately for this variant). The components of vector $\underline{V}$ are thus:

$$V_r=\frac{r\left(\frac{1}{2}r^2+z^2\right)^{3/2}}{r^2+4z^2} \qquad V_z=\frac{2z\left(\frac{1}{2}r^2+z^2\right)^{3/2}}{r^2+4z^2}$$

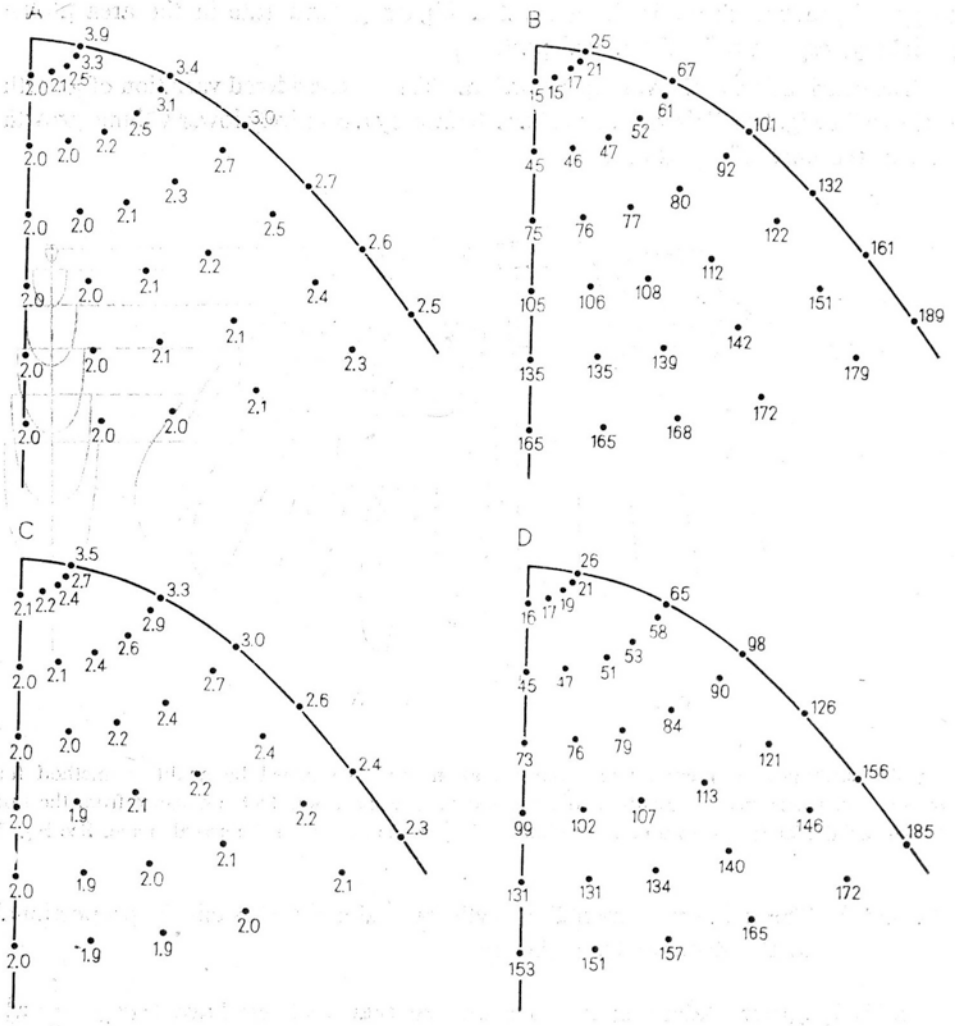


Fig. 5. Distribution of rates of growth in volume. The rates are indicated for the nodes of the net shown in Fig. 1. A and B — obtained by analytical method for variant 1 and 2, respectively, C and D — obtained by graphical method for variant 1 and 2, respectively

The direction cosines of the displacement line are also the same as in the previous case. Using formulas (5—14) for growth rates we obtain:

$$RERG_{1\,(per)} = \frac{\left(\frac{1}{2}r^2+z^2\right)^{1/2}}{(r^2+4z^2)^3}(r^6+11r^4z^2+44r^2z^4+64z^6)$$

$$RERG_{1\,(ant)} = \frac{\left(\frac{1}{2}r^2+z^2\right)^{1/2}}{(r^2+4z^2)^3}(r^6+8r^4z^2+20r^2z^4+16z^6)$$

$$RERG_{l\,(lat)} = \frac{\left(\frac{1}{2}r^2+z^2\right)^{3/2}}{r^2+4z^2}$$

$$RERG_{l\,(rad)} = \frac{\left(\frac{1}{2}r^2+z^2\right)^{1/2}}{(r^2+4z^2)^2}(r^4+7r^2z^2+4z^4)$$

$$RERG_{vol} = \frac{\left(\frac{1}{2}r^2+z^2\right)^{1/2}}{(r^2+4z^2)^2}\left(\frac{5}{2}r^4+14r^2z^2+24z^4\right)$$

The results of calculations are summarized in Figs 4 and 5 B. As could be expected, there is a marked increase of relative elemental growth rates of all kinds with the distance from the tip. At the very tip the rates are zero. The linear rate on the surface near the tip is generally low, but nearly twice faster in the meridional than in the latitudinal direction. This anisotropy is due to the fact that there is a fast change of meridional growth rate with distance from the tip, while latitudinal growth rate changes slower (the latter depends rather on the velocity of displacement of the latitudinal circle along which it is measured than on the local meridional growth rate). The anisotropy of growth on the dome surface becomes more pronounced as the distance from the tip increases. In the axial plane the anisotropy is more pronounced in the core than at the periphery. It is worth to noting that the periclinal growth rate is nearly the same for all points of an orthogonal trajectory of displacement lines, this proving the validity of formula (19a). However, the periclinal growth rate at the same level, i.e. at the same z, increases with the distance from the axis. On the transverse plane the growth rate in latitudinal direction is slightly higher than in the radial direction. Both rates increase with the distance from the axis and from the tip. Growth rates in area higher at the periphery of the dome than in its core for all planes. The same is observed for growth in volume, Fig. 5B.

## 2. Graphical approach

We have elaborated by the graphical method the same variants of growth as previously described analytically, using the same units. The results obtained are practically the same as those from the analytical procedure. To illustrate the similarity, the results for volume growth rate are shown in Fig. 5C, D. Our conclusion from the comparison of analytical and graphical results is that the graphical method is good enough to be used in practice. This is important because in practice we shall not have the geometry of a dome and of $G(z_0)$ in analytical form. By using the graphical method we have made calculations for variant 3 in which the growth rate along the axis and corresponding $V(z_0)$ are shown in Fig. 6A. The aim was to see the pattern of growth rate in a case more realistic than in the previous variants.

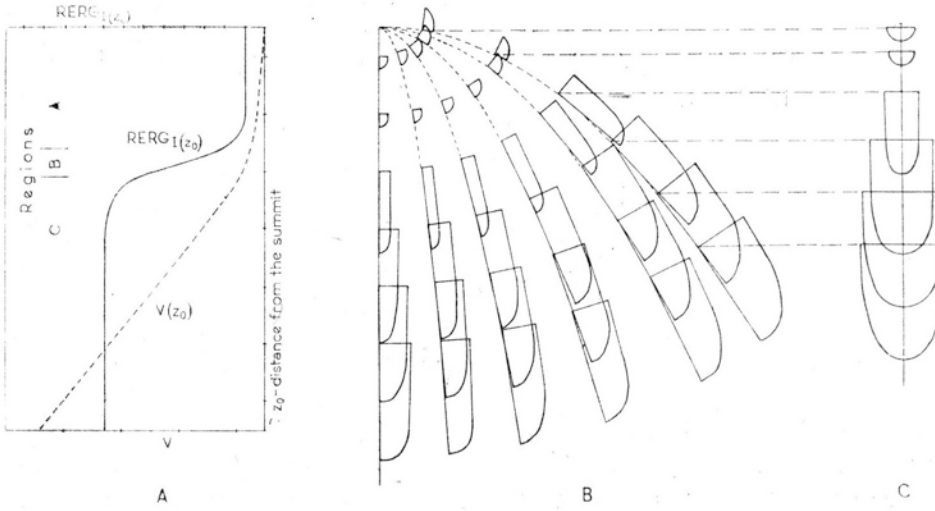


Fig. 6 Distribution of growth rates — linear and in area — obtained by graphical method for variant 3 characterized by growth rate along the axis as shown in A. B — in axial plane, C — on the surface of the apical dome. See Fig. 3

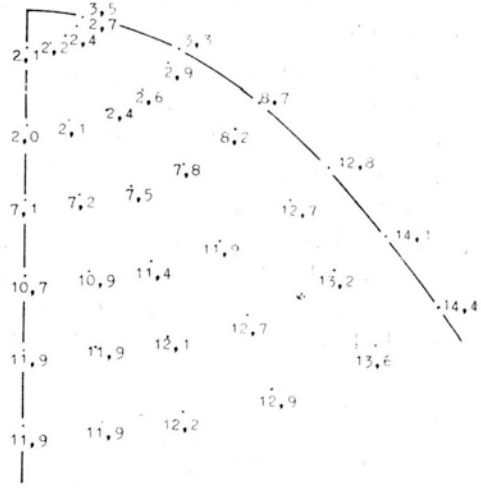


Fig. 7 Distribution of rates of growth in volume for variant 3

The results are summarized in Fig. 6B, C and 7. There is nearly isotropic growth n the upper part of the dome similarly as in variant 1 (in the region where the ssumed growth rate along the axis is constant). Growth in the basal part is strongly nisotropic, even more than in variant 2, which is obviously due to a very rapid ncrease of growth along the z-axis in region B, Fig. 6A. Very interesting is the distribution of volume growth rate, namely, this rate is generally low in the summital part, but there is a clear depression of the rate in the core of this part.

### 3. Temporal expansion of the dome

The relation between the position of a material element on the axis and the time, defined by equation (15) is $t-t_0=\ln\frac{z}{z_0}$ and $t-t_0=\frac{2}{z_0}-\frac{2}{z}$ for variant 1 and 2, respectively.

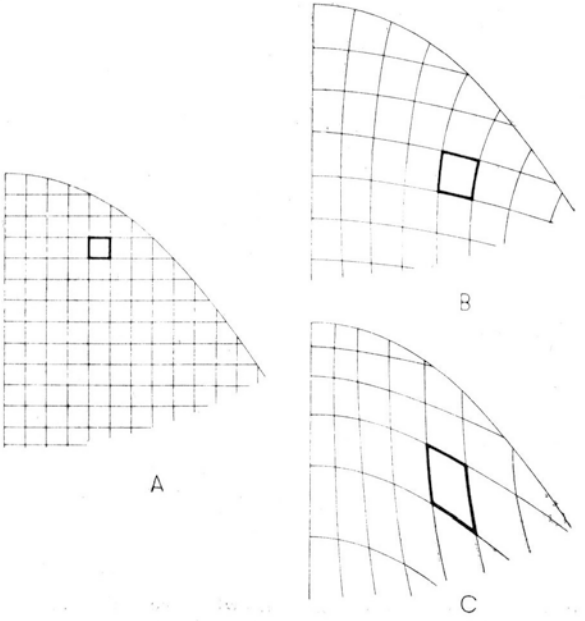


Fig. 8. Deformation of a net which originally was quadratic as shown in A. B — for variant 1 (linear growth rate along the axis constant), C — for variant 2 (linear growth rate along the axis increases proportionally to the distance from the tip). To facilitate comparison one mesh is delineated by heavy line. The time interval between states A and B is different from that between A and C

Fig. 8 illustrates the deformation of a net which originally was quadratic. In variant 1 the net is deformed so that the lines which were originally parallel to the axis tend to diverage in respect to the tip, while in variant 2 there is a tendency to convergence. It should be noted that in both variants the horizontal lines become convex towards the tip, i.e. the dome grows so that each transverse plane in it tends to protrude toward the tip. In variant 2 the net is as if almost attached close to the tip and drawn along the displacement lines downwards.

Fig. 9 shows deformation of the cell wall net on the axial plane. The net looks originally as in Fig. 9A, while after some time of growth—as in Fig. 9B and 9C in the two variants, respectively. One can imagine that, when the mesh of the net increases it becomes partitioned so as to keep the average size constant. In variant 1 th, partitions will be oriented as often anticlinally as periclinally, while in variant 2 there ts a high prevalence of anticlinal partitions. Thus, in variant 1 there is a tendence o a massive type of cell arrangement, while in variant 2—to a rib type.

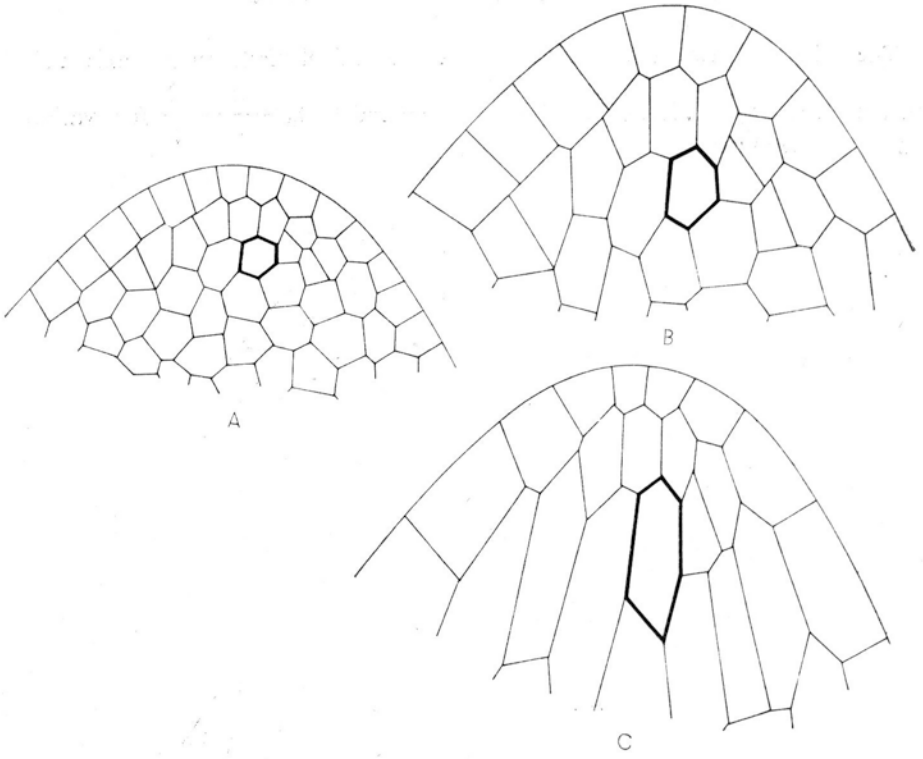


Fig. 9 Deformation of a cell wall net in axial plane
A — original state, B — for variant 1 (linear growth rate along the axis constant), C — for variant 2 (linear growth rate along the axis increases proportionally to distance from the tip). One "cell" is marked by heavy line to facilitate comparison

## DISCUSSION

This paper shows how the distribution of growth rates can be evaluated in the apical dome if data on the geometry of the dome including the pattern of displacement lines and linear growth rates along one longitudinal direction are available. The geometry of the dome, its shape and behavior in time can be obtained from anatomical studies. From the latter we can also infer the pattern of displacement lines (Schüepp, 1966). The data on the linear growth rate along the meridional line on the surface may be obtained from direct measurements of displacement velocity of elements on the dome surface, though such measurements have not been reported in the literature. They may also be inferred from determination of the sizes of cell complexes in a stationarily growing apex or from the distribution of the mitotic index.

In the literature a lot of partial data can be found pertinent to the problem of the growth pattern in shoot apical meristems, but they are only used in estimating some aspects of this pattern. A most complete survey of these data was done by

Schüepp (1966). However, there is no paper in which these data are utilised to give a complete picture of the growth pattern in a shoot apex. In the present paper such a complete picture is offered, but only for a model of a shoot apex. We believe, however, that this method may be used for a real dome. Our preliminary trials indicate that the method may be extended to cases where the shape of the dome is not stationary owing to the crossing of the dome surface by displacement lines, or even to a temporary change of the pattern of displacement lines.

The general picture of the growth of a shoot apex constructed from the literature (Lyndon, 1976) roughly fits within the range of variants 1 and 2 considered in this paper. Variant 3 seems to be the most realistic in the case of the corpus of the shoot apex in seed plants. If this is the case, the low rate of growth in the subapical part and the depression of the growth rate in the core of this part deserve attention. Such a pattern of growth may be related to the cytohistological zonation in the apices of seed plants. Especially the zone of central mother cells in shoot apices of gymnosperms and in many dicotyledonous plants seems to be related to the subapical depression of growth rate.

The pattern of displacement lines in many real apices probably differs in details from the parabolic ones assumed in this paper. In apices which have a tunica-corpus organization the displacement lines within the tunica run parallel to the dome surface (the anticlinal growth rate is null within the tunica) and only those in the corpus converge to one point (Schüepp, 1966). The partern of displacement lines assumed in this paper obviously does not fit the presence of a tunica. In the case of an apex with tunica-corpus organization, this pattern refers to the corpus alone. In such a case, however, we can estimate the growth rate in the tunica; the volume growth rate of the tunica must be equal that of the area growth rate on the corpus surface ($RERG_{I\,(ant)}=0$ in tunica). This means that the organization tunica-corpus depresses the rate of volume growth in the apical part of dome containing the cells of the "germ line". Our modeling allows to estimate that this rate is lowered to half of that which would occur without tunica-corpus organization.

The senior author has put forward the hypothesis (Hejnowicz, 1980 b) that the organization and growth pattern of shoot apex protects the cells on the "germ line" from errors appearing during DNA replication in vegetative development and which are more probable in cells occurring on the apex surface than in those located inside. This protection is achieved by: 1. lowering the rate of growth in the apical region of the shoot apex during the vegative phase of development; 2. positioning of the "germ line" under the surface cells, this being posible owing to the tunica-corpus organization. The two-layered tunica in which the second layer belongs to the "germ line" serves not only the 2-nd point, but also additionally lowers the frequency of divisions of its cells.

The parabolic lines in the corpus itself probably differ from parabolic ones. Judging by the arrangement of cells, it seems that the displacement lines in the axial part of the corpus run almost parallel to the axis already on the level of the mother cell zone. This means that the radial (anticlinal) growth rate close to the

axis is lower than in our models, and thus, on a compensatory basis, the radial (anticlinal) growth rate in the peripheral parts is higher. If this is the case, the slight depression of growth rate in the core of the subapical part, occurring in variant 3 would be more pronounced.

The knowledge of the growth rate distribution in the shoot dome is important in many aspects. One is the ontogenic drift of cells and of the populations which develop from them. The drift—the relation between cell position and time—may be calculated if the distribution of growth rate is known. An other aspect is the morphogenesis of the apex. The growth rate distribution is the basis for morphogenesis. A very important aspect is the distribution of rate of different processes occurring in the apex. To calculate this distribution we need the field of velocity of cell displacement besides the spatial variation of the quantity studied (Silk and Erickson, 1978, 1979).

## REFERENCES

Erickson, R. O., 1966. Relative elemental rates and anisotropy of growth in area: a computer programme. J. Exp. Bot. 17:390-403.

Erickson R. O., 1976. Modeling of plant growth, Ann. Rev. Plant Physiol. 27: 407—434.

Hejnowicz Z., 1980a. Vector and scalar field in modeling of plant organ growth, J. theor. Biol. (in press).

Hejnowicz Z., 1980b. Anatomia i histogeneza roślin naczyniowych PWN, Warszawa.

Lyndon R. F., 1976. The shoot apex, [In:] Cell division in higher plants, M. M. Yeoman (Ed. 285—314, Academic Press, London.

Schüepp O., 1966. Meristeme, Wachstum und Formbildung in dem Teilungsgeweben höheren Pflanzen, Birkhauser Verlag, Basel

Silk W. K. and Erickson R. O., 1978. Kinematics of hypocotyl curvature, Amer. J. Bot. 65: 310—319

Silk W. K. and Erickson R. O., 1979. Kinematics of plant growth, J. theor. Biol. 76: 481—501.

*Authors' address*:
*Prof. dr. Zygmunt Hejnowicz and dr. Jerzy Nakielsk)*
*Department of Biophysics and Cell Biology*
*Silesian University*;
*Jagiellońska 28*; *40-032 Katowice, Poland*

## *Modelowanie wzrostu wierzchołka pędu*

Streszczenie

Podczas wzrostu wierzchołka elementy siatki ścian komórkowych przesuwają się z określonymi pla danej części prędkościami. Istnieje więc pole wektorowe prędkości przesunięć V. Matematyczdna aaliza tego pola pozwala znaleźć rozmieszczenie szybkości wzrostu (RERG): odcinka linii w downlnym kierunku, elementu powierzchni na dowolnym przekroju, elementu objętości w różnych ounktach wierzchołka. W niniejszej pracy pokazujemy, jak można to zrobić w oparciu o znajomość

geometrii wierzchołka i szybkości wzrostu liniowego wzdłuż jednej z linii przesunięć a mianowicie wzdłuż osi. Zarówno geometrię (kształt wierzchołka i wzór linii przesunięć), jak i szybkość wzrostu liniowego wzdłuż osi można wyznaczyć empirycznie. Rozpatrujemy kilka możliwych wariantów szybkości wzrostu liniowego na osi ($RERG_{l(z_0)}$):

1. gdy $RERG_{l(z_0)}$ jest stałe na osi
2. gdy $RERG_{l(z_0)}$ jest proporcjonalne do odległości od szczytu
3. gdy $RERG_{l(z_0)}$ jest zadaną graficznie kombinacją dwóch poprzednich wariantów. Obliczenia przeprowadziliśmy dla wierzchołka o kształcie paraboloidy obrotowej z parabolicznymi liniami przesunięć dwoma metodami: analityczną — opartą na równaniach parabol, i graficzną — wykorzystującą jedynie zależności wynikające z rysunku. Dla obu metod uzyskaliśmy niemal jednakowe rezultaty, wykazując tym samym przydatność metody graficznej. Rezultaty obliczeń uzyskane dla wariantu 3 są zbieżne z wynikami badań empirycznych wierzchołków pędu roślin nasiennych z charakterystyczną dla nich małą szybkością wzrostu w części przyszczytowej oraz depresją szybkości wzrostu objętościowego wewnątrz tej części. Wyliczyliśmy również czasowy przebieg ekspansji siatki ścian komórkowych.